

Revisiting the Synthesis and Elucidating the Structure of Potassium Cyclopentadienyldicarbonylruthenate $\text{K}[\text{CpRu}(\text{CO})_2]$

Kai F. Kalz,[†] Nicole Kindermann,[†] Sheng-Qi Xiang,[‡] Andreas Kronz,[§] Adam Lange,[‡] and Franc Meyer^{†*}

[†] Institute of Inorganic Chemistry, Georg-August-University Göttingen, Tammannstrasse 4, D-37077 Göttingen, Germany

[‡] Max Planck Institute for Biophysical Chemistry, Am Fassberg 11, D-37077 Göttingen, Germany

[§] Geowissenschaftliches Zentrum, Georg-August-University Göttingen, Goldschmidtstrasse 1, D-37077 Göttingen, Germany

Supporting Information

Contents

1. Methods and Materials.....	2
2. Synthetic Procedures.....	2-3
2.1. Synthesis of $[\text{CpRu}(\text{CO})_2]_2$ (Rp_2)	2
2.2. Synthesis of $\text{K}[\text{CpRu}(\text{CO})_2]$ (KRp) and the Black Solid.....	3
2.3. ^{13}C -Labeled Compounds.....	3
3. X-Ray Crystallography	4
4. IR Spectroscopy	5-6
4.1. Solution State IR Spectroscopy of the Black Solid	5
4.2. ATR IR Spectroscopy and ^{13}C Labeling.....	6
5. UV/Vis Spectroscopy.....	7-8
5.1. Solution State UV/Vis Spectroscopy of KRp	7
5.2. Solid State UV/Vis Spectroscopy	8
6. Solid State ^{13}C MAS NMR Spectroscopy	9-11
6.1. Cross Polarization Spectra of KRp and the Black Solid.....	9
6.2. Direct Excitation Spectrum and Quantification.....	10
7. Elemental Analysis and Electron Microprobe Analysis (EMPA)	12
8. References.....	13

1. Methods and Materials

All reactions were carried out under argon (dried over phosphorous pentoxide on solid support [SICAPENT[®], Merck] and liberated from traces of oxygen by a heated copper catalyst) using standard Schlenk techniques or in a glovebox (MBRAUN LabMaster) under a nitrogen atmosphere. Solvents were dried and degassed by standard procedures before use. Chemicals were purchased from Aldrich, Acros, Merck, Deutero or ABCR. Cyclopentadiene was prepared by cracking dicyclopentadiene over iron filings and distillation using a fractionating column. ¹³C-enriched CO gas (99 % ¹³C) was purchased from Euriso-Top.

Solution-state NMR spectra were recorded on Bruker AVANCE 300 or 500 instruments at 25 °C. Chemical shifts (δ) are given in ppm and are referenced to the solvent residual signals.¹ Solid state NMR experiments were carried out on a Bruker AVANCE 400 spectrometer equipped with a (¹H, X, Y) triple resonance 4 mm MAS probe. The ¹³C chemical shifts were referenced externally to adamantane.

IR spectra were recorded using a Cary 630 FTIR spectrometer (Agilent) placed in a glovebox (MBRAUN UNILab, argon atmosphere) with DialPath and Diamond ATR accessory. IR bands were labeled according to their relative intensities with s (strong), m (medium), w (weak) and sh (shoulder).

UV/Vis spectra were recorded with a Varian Cary 5000 UV/Vis/NIR instrument using sealable quartz cuvettes for solutions or a Praying Mantis sampling kit for solid samples.

Elemental analyses (CHN) were performed on an Elementar 4.1 vario EL 3 element analyzer. The ruthenium content was determined photometrically by a Perkin-Elmer Lambda 2 UV/Vis spectrometer after pressure digestion with HNO₃ and the potassium content was obtained using a Thermo Scientific IRIS Intrepid II instrument.

2. Synthetic Procedures

2.1 Synthesis of [CpRu(CO)₂]₂ (Rp₂)

The ruthenium dimer Rp₂ was synthesized according to a modified literature procedure.² Triruthenium dodecacarbonyl Ru₃(CO)₁₂ (1.7 g, 2.7 mmol, 1.0 eq.), dry and deoxygenated *n*-heptane (80 mL) and freshly distilled cyclopentadiene (4.1 g, 5.3 mL, 62 mmol, 23 eq.) were heated for 2 h at reflux in a two-necked round-bottomed flask under an argon atmosphere. The glass stopper was then removed and the volume of solvent was reduced to roughly 10 mL under a brisk flow of argon before adding again a volume of 110 mL of unpurified *n*-heptane directly from the reagent bottle. The solution was heated for a further 3 h. Upon standing over night, the product crystallized from the reaction mixture. In order to complete crystallization, an additional amount of 30 mL of unpurified *n*-heptane was added to the reaction mixture and the flask was kept at 0 °C for 1 d. Decantation, washing the crystals with *n*-pentane and drying in vacuo afforded the product as orange needles (1.3 g, 3.0 mmol, 74 %).

¹H NMR (300 MHz, CD₃CN): δ (ppm) = 5.36 (s, 5 H; Cp).

¹³C NMR (75 MHz, CD₃CN): δ (ppm) = 221 (CO), 91 (Cp).

IR (MeCN): $\tilde{\nu}$ (cm⁻¹) = 1997 (s), 1959 (m), 1937 (sh), 1776 (s).

IR (KBr): $\tilde{\nu}$ (cm⁻¹) = 1948 (s), 1771 (s).

2.2 Synthesis of K[CpRu(CO)₂] (KRp) and the Black Solid

To a solution of Rp₂ (0.50 g, 1.1 mmol, 1.0 eq.) in THF (20 mL), potassium tri-*sec*-butylborohydride (K-Selectride[®], 1 M in THF, 6.7 mL, 6.7 mmol, 6.1 eq.) was added and the resulting mixture was heated to 40 °C for 6 h. After a short time the initially orange solution turned darker and precipitation of a finely dispersed black solid was observed. Stirring of the mixture was continued over night and the precipitate was isolated by filtration and subsequent washing with THF (2 x 5 mL) and MeCN (2 x 10 mL). Exhaustive drying of the solid in vacuo afforded a black material (0.10 g). Toluene (60 mL) was added to the filtrate and after 1 d the resulting crystals were collected by decantation, washed with toluene and dried in vacuo. By this method, KRp was obtained as yellow crystals (0.24 g, 0.90 mmol, 41 %). Crystals suitable for X-ray diffraction were obtained by layering a THF solution of the compound with toluene. Caution is required when handling the compound outside a glovebox as any exposure to air immediately destroys the crystals.

Analytical data of KRp (the data for the black solid can be found in sections 4-7):

¹H NMR (300 MHz, CD₃CN): δ (ppm) = 4.83 (s, 5 H; Cp).

¹H NMR (300 MHz, DMSO-d₆): δ (ppm) = 4.68 (s, 5 H; Cp).

¹³C NMR (75 MHz, CD₃CN): δ (ppm) = 216 (CO), 80 (Cp).

¹³C NMR (75 MHz, DMSO-d₆): δ (ppm) = 215 (CO), 80 (Cp).

IR (MeCN): $\tilde{\nu}$ (cm⁻¹) = 1888 (s), 1803 (s).

IR (THF): $\tilde{\nu}$ (cm⁻¹) = 1895 (s), 1812 (s).

IR (DMSO): $\tilde{\nu}$ (cm⁻¹) = 1882 (s), 1796 (s).

Elemental Analysis: Calcd. (%) for C₇H₅KO₂Ru: C 32.18, H 1.93. Found: C 32.17, H 2.05.

2.3 ¹³CO-Labeled Compounds

¹³CO-enriched triruthenium dodecacarbonyl was obtained according to a modified literature procedure from Darensbourg and coworkers.³ Commercially available Ru₃(CO)₁₂ (1.0 g, 1.6 mmol) dissolved in a mixture of THF (90 mL) and MeOH (50 mL) and catalytic amounts of KOMe (0.1 M in MeCN/toluene, 0.2 mL, 0.02 mmol) were placed in a 500 mL Schlenk flask and the mixture was degassed by repeated freeze-thaw cycles. The flask was charged with an atmosphere of ¹³CO gas (1 bar) and the mixture was stirred for 3 h at 50 °C. Stirring was continued over night. After this, the atmosphere of ¹³CO was renewed and the mixture was stirred for another 5 h at 50 °C. The solvent was removed in vacuo and the raw product was extracted with warm *n*-hexane. Filtration and removal of the solvent afforded the ¹³CO-enriched Ru₃(CO)₁₂ which was directly used in the synthesis of ¹³CO-enriched Rp₂ (¹³CO-Rp₂) analogously to the preparation of the non-labeled compound described in section 2.1. From NMR spectroscopy of ¹³CO-Rp₂ in comparison with the unlabeled compound, the ¹³C content in the CO molecules was estimated to be at least 90 %. Subsequent reductive cleavage according to section 2.2 gave the ¹³CO-enriched metallate and the ¹³CO-enriched black solid.

3. X-ray Crystallography

X-ray data were collected on a STOE IPDS II diffractometer with an area detector (graphite monochromated Mo-K α radiation, $\lambda = 0.71073$ Å) by use of ω scans at 133 K (Table S1). The structure was solved by direct methods and refined against F^2 using all reflections with SHELX-2013.⁴ All non-hydrogen atoms were refined anisotropically. All hydrogen atoms were placed in calculated positions and assigned to an isotropic displacement parameter of 1.2 / 1.5 $U_{eq}(C)$. Face-indexed absorption corrections were performed numerically with the program X-RED.⁵

CCDC 983836 (KRp·THF) contains the supplementary crystallographic data for this paper. These data can be obtained free of charge from The Cambridge Crystallographic Data Centre via http://www.ccdc.cam.ac.uk/data_request/cif.

Table S1: Crystal data and refinement details.

	KRp·THF
empirical formula	C ₁₁ H ₁₃ KO ₃ Ru
formula weight	333.38
T [K]	133(2)
crystal size [mm ³]	0.325×0.288×0.124
crystal system	orthorhombic
space group	<i>Pbca</i>
a [Å]	8.7374(17)
b [Å]	11.492(2)
c [Å]	24.169(5)
α [°]	90
β [°]	90
γ [°]	90
V [Å ³]	2426.9(8)
Z	8
ρ [g/cm ³]	1.825
$F(000)$	1328
μ [mm ⁻¹]	1.623
T_{min} / T_{max}	0.2958 / 0.7075
θ -range [°]	1.685 - 25.705
hkl -range	$\pm 10, \pm 13, \pm 29$
measured refl.	21384
unique refl. [R_{int}]	2284 [0.0982]
observed refl. ($I > 2\sigma(I)$)	2029
data / restraints / param.	2284 / 0 / 145
goodness-of-fit (F^2)	1.073
$R1, wR2$ ($I > 2\sigma(I)$)	0.0249, 0.0637
$R1, wR2$ (all data)	0.0300, 0.0659
resid. el. dens. [e/Å ³]	-0.585 / 0.522

4. IR spectroscopy

4.1 Solution State IR Spectroscopy of the Black Solid

The black solid dissolves only (and only partly) in very polar solvents. Figure S1 depicts the solution state IR spectra of the compound in DMSO, DMF and MeOH obtained after filtration (Sartorius PTFE syringe filter, 0.45 μm), in comparison with the IR spectrum of KRp in DMSO. The finding that the IR bands of KRp (1883 and 1795 cm^{-1}) are also present in the spectra of the black solid suggests that Ru/Cp/CO are components of the black solid, and that the Rp^- unit is formed after treatment with the above solvents. The unusually broad IR bands may indicate that an association phenomenon is operative in solutions of the black solid. The degree of association and hence the bandshape obviously depend on the polarity of the applied solvent. When MeOH is used, the solid dissolves completely and a yellow solution is obtained which exhibits IR bands significantly different from KRp (2026 and 1963 cm^{-1}). Although the unusual bandshape remains, the position of the bands now closely resembles the IR bands reported for the metal hydride $\text{HRu}(\text{Cp})(\text{CO})_2$ (HRp).⁶ It is likely that the black solid gets protonated by the protic solvent MeOH.

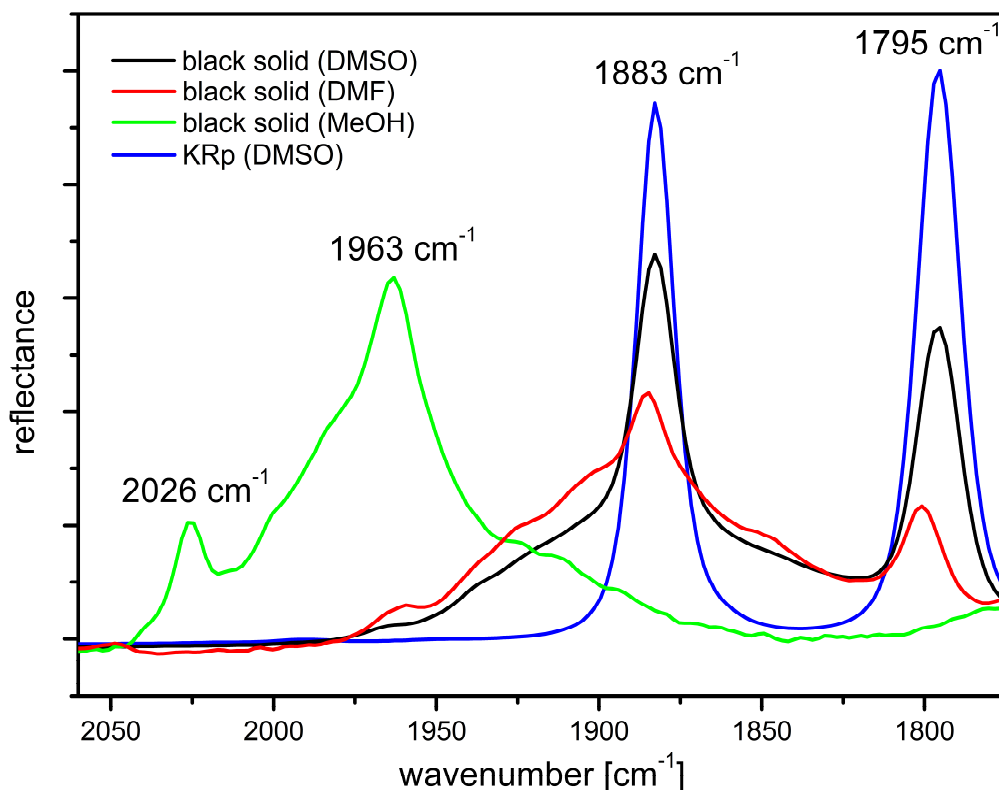


Figure S1. IR spectrum of the black solid dissolved in DMSO (black line), DMF (red line) and MeOH (green line) as well as the IR spectrum of KRp in DMSO (blue line) for comparison.

4.2 ATR IR Spectroscopy and ^{13}C O Labeling

ATR IR spectra of the black solid were recorded on a Cary 630 FTIR spectrometer (Agilent) under inert conditions. The spectra display unusually broad signals and also the position of the bands is atypical for CO molecules in organometallic compounds. If one compares the spectrum of the black solid and the ^{13}C O-enriched black solid, one notices a shift for specific bands to lower wavenumbers in the labeled compound. This is expected for bands caused by vibrations with significant contribution of CO molecules. As depicted in Figure S2, this is particularly true for the broad bands centered at 1815 and 1536/1468 cm^{-1} and hence it can be concluded that CO ligands are present in the black solid. Carbonyl stretching frequencies as low as 1612 cm^{-1} have been reported before for ruthenium clusters⁷ and in some anionic osmium carbonyl complexes ion pairing effects between CO molecules and K^+ have been identified as a reason for low CO stretching frequencies (1625 cm^{-1}).⁸ Similar effects may also be operative in the present case.

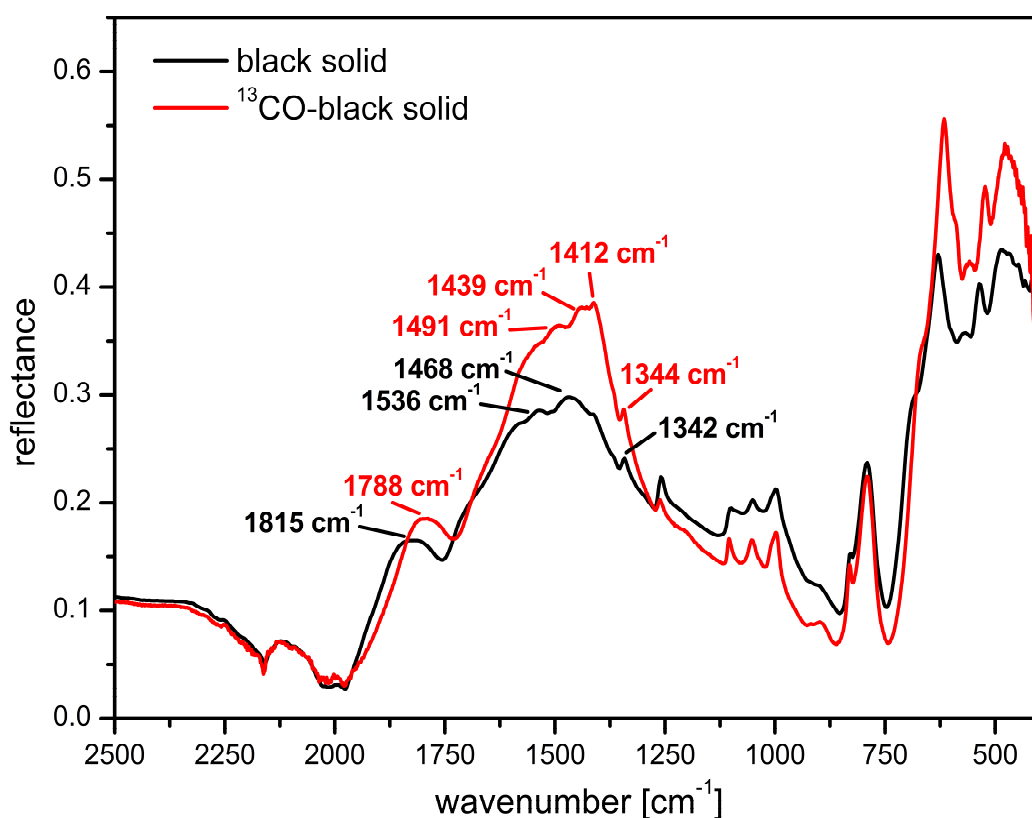


Figure S2. ATR IR spectrum of the black solid (black line) and the ^{13}C O-enriched compound (red line). The broad bands shift to smaller wavelengths in the labeled compound.

5. UV/Vis Spectroscopy

5.1 Solution State UV/Vis Spectroscopy of KRp

The solution state UV/Vis spectra of KRp were recorded with a Varian Cary 5000 UV/Vis/NIR instrument using sealable quartz cuvettes. Solutions of the metallate were prepared in a glovebox directly before the measurement. As the absorptions were only visible as shoulders, the spectra were transformed into energy plots and fitted with Gaussian functions using the *Fityk* program.⁹ Figure S3 depicts the recorded spectrum at a 0.7 μM concentration. Deconvolution of the spectrum gave three absorptions at 242 ($\epsilon = 3200 \text{ L mol}^{-1} \text{ cm}^{-1}$), 281 ($\epsilon = 4300 \text{ L mol}^{-1} \text{ cm}^{-1}$) and 331 nm ($\epsilon = 1200 \text{ L mol}^{-1} \text{ cm}^{-1}$).

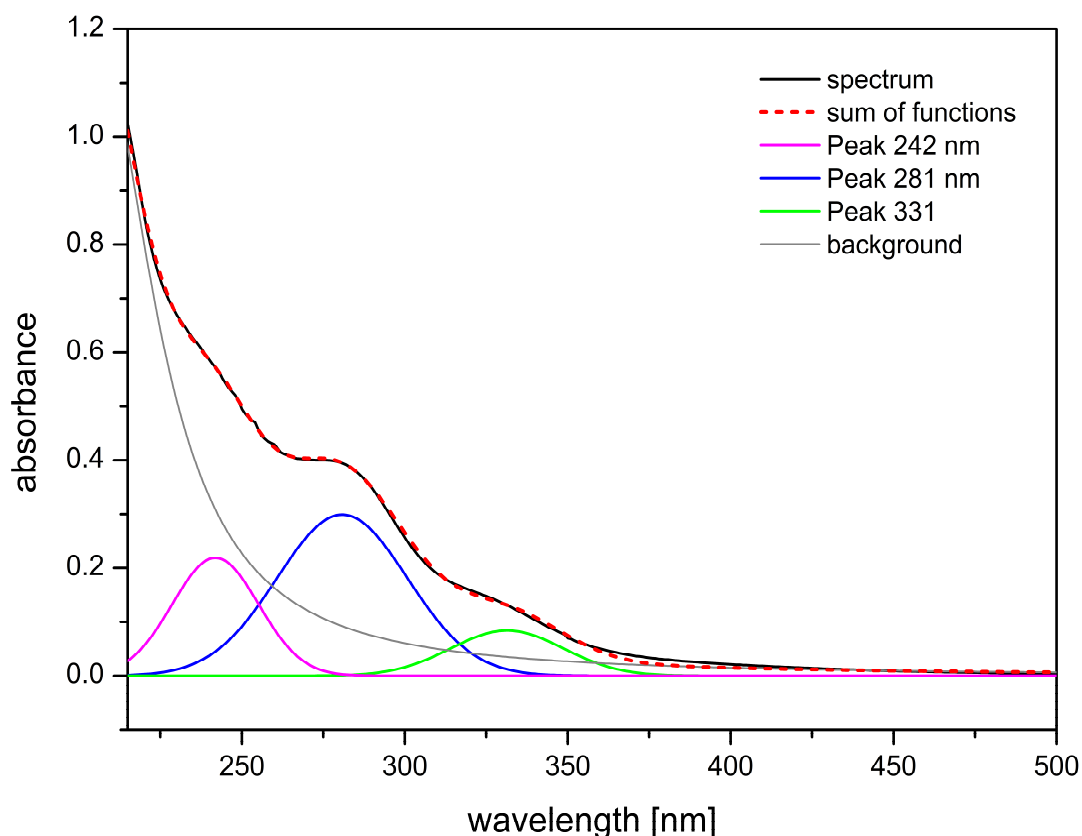


Figure S3. UV/Vis spectrum of KRp in THF showing three absorptions at 242, 281 and 331 nm. Absorption bands were obtained after deconvolution with the *Fityk* program.⁹

5.2 Solid State UV/Vis Spectroscopy

Solid state UV/Vis spectra of KRp and the black solid were recorded with a Varian Cary 5000 UV/Vis/NIR instrument equipped with a Praying Mantis sampling kit for solid samples. Figure S4 shows the solid state UV/Vis spectrum of KRp and the black solid. From the continuous absorption over a large wavelengths range, two absorptions at 236 and 284 nm are clearly discernible. These two absorptions are very similar to the absorptions found for KRp in the solid state (236 and 281 nm) and are similar to the absorptions at 242 and 281 nm observed in THF solution spectra of KRp (see Figure S3).

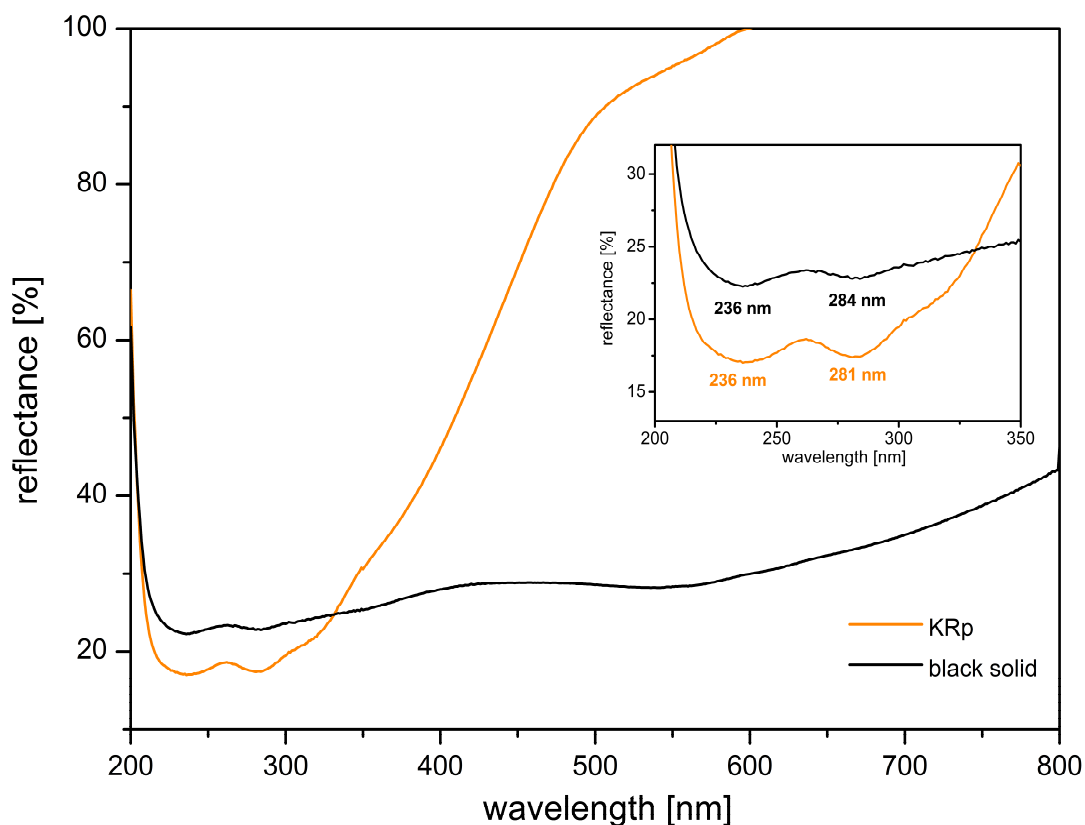


Figure S4. Solid state UV/Vis spectrum of KRp (orange line) and the black solid (black line). The absorptions in the UV region are similar and also comparable to the solution spectra of KRp.

6. Solid State ^{13}C MAS NMR Spectroscopy

The employed MAS rates were 9, 11 and 12 kHz. Typical 90° pulse lengths were $3\ \mu\text{s}$ for proton and $5\ \mu\text{s}$ for carbon. In carbon direct excitation experiments, interscan delays were set to 240 s to avoid saturation. The ^1H - ^{13}C cross polarization contact time was 1.3 ms. The interscan delay in CP experiments was set to 2.5 s. In all cases, the ^1H decoupling field strength was 80 kHz during acquisition.

6.1 Cross Polarization Spectra of KRp and the Black Solid

Figure S5 depicts the ^{13}C CP/MAS NMR spectrum of KRp at a spinning rate of 9 (yellow line) and 11 kHz (blue line). Besides the spinning sidebands, only two signals at 218 and 87 ppm are observed characterizing the terminal CO molecules and the cyclopentadienyl ring, respectively.

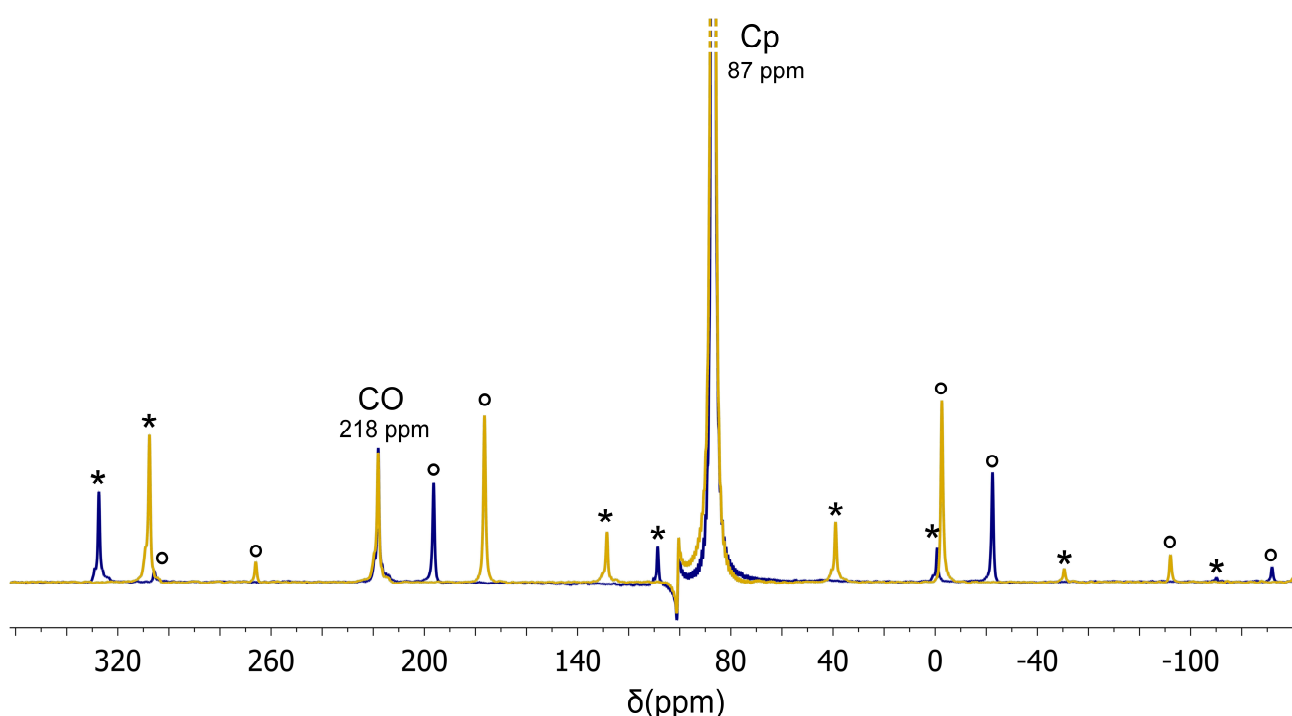


Figure S5. ^{13}C CP/MAS spectra of KRp at 9 kHz (yellow) and 11 kHz (blue) spinning rate showing terminal CO molecules (218 ppm) and the Cp ring (87 ppm). Spinning sidebands of the terminal CO signal are marked with an asterisk (*), sidebands of the Cp ring with a circle (o).

In comparison with the solid state NMR spectra of KRp, the signals especially of the CO molecules in the ^{13}C CP/MAS spectra of the black solid are significantly broader. A possible explanation for this could be the crystalline nature of the KRp sample, but also paramagnetic impurities, anisotropic motion or incomplete scrambling of the carbonyl ligands in the sample of the black solid might lead to broad signals. As the signal intensity of the CO carbon atoms was very low, a ^{13}C O-enriched sample of the black solid was prepared (see section 2.3). In the ^{13}C CP/MAS spectra of this sample, the CO signals were far better resolved, albeit the signals were still very broad. Figure S6 shows spectra of the ^{13}C O-

enriched compound at different spinning rates. It is evident that two different kinds of CO molecules exist, namely bridging (280 ppm) and terminal COs (215 ppm). The chemical shift anisotropy (CSA) is larger for the terminal CO molecules and hence more intensity is distributed into the spinning sidebands of this signal. The origin of the signal at 173 ppm and of the (partly obscured) signal at ~4 ppm could not be resolved unambiguously. The varying intensity of the signals in different samples hints at impurities, the one at 4 ppm possibly being due to silicon grease as analytical methods revealed trace amounts of Si in the black solid (see below). It cannot be fully excluded that a third CO species is present in the black solid giving rise to the signal at 173 ppm – although the upfield chemical shift is rather unusual for CO ligands – since the signal exhibits a gain in intensity in the ^{13}C -enriched compound. Although quantification was difficult because of problematic integration in the unlabeled compound, this gain in intensity seems to be lower than in the case of the bridging and terminal COs.

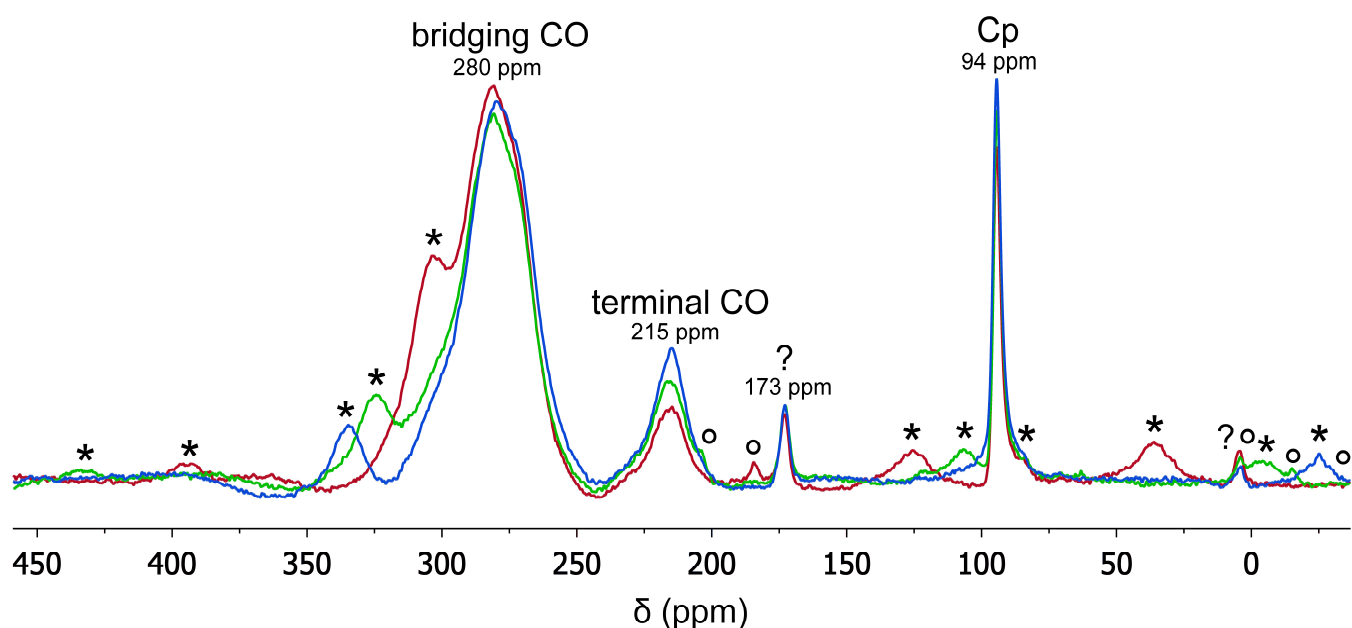


Figure S6. ^{13}C CP/MAS spectra of the ^{13}C -enriched black solid at 9 kHz (red), 11 kHz (green) and 12 kHz (blue) spinning rate showing bridging (280 ppm) and terminal CO molecules (215 ppm). First and second order sidebands of the terminal CO signal are marked with an asterisk (*), first order sidebands of the Cp ring (94 ppm) with a circle (o). The two signals marked with a question mark could not yet be assigned, but are presumably due to impurities.

6.2 Direct Excitation Spectrum and Quantification

The ratio between bridging and terminal CO molecules was determined by integration of a ^{13}C MAS spectrum of the ^{13}C -enriched black solid which was acquired by a direct excitation method. The spectrum at a spinning rate of 12 kHz (Figure S7) allows for integration and subsequent determination of a ratio of the CO signals. The intensity of the spinning sidebands of the terminal CO signal was taken into account. Furthermore, the integral of the upfield first order spinning sideband of the terminal CO signal was estimated by fitting two Gaussian functions to the peak at 94 ppm (sideband and Cp signal). For the black solid, a ratio of 3.1:1.0 for the bridging vs. terminal CO molecules was calculated. As can be seen in Figure S7, the intensity of the peaks at 173 (impurity?) and 94 ppm (Cp) decrease relative to the CO signals, hence they profit from the cross polarization method significantly more than bridging and

terminal CO signals. This indicates that protons can be found in the vicinity of the respective carbon atoms.

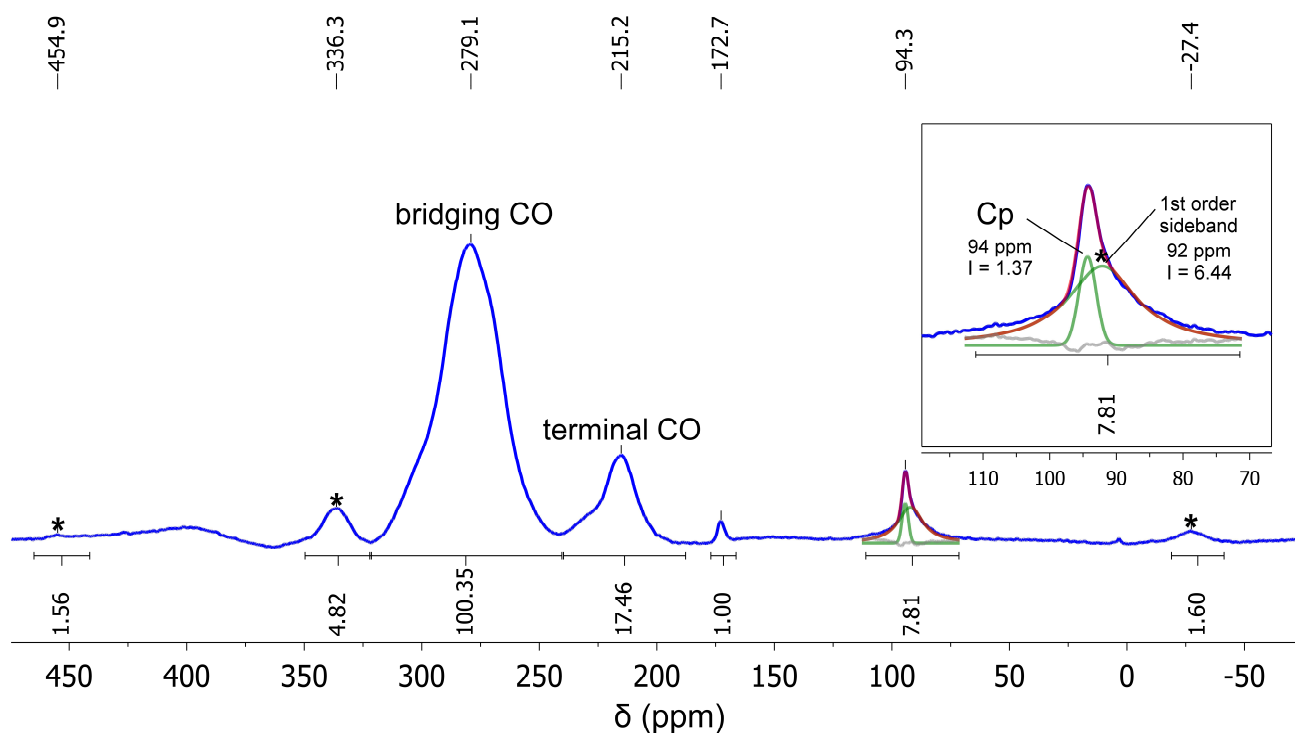


Figure S7. ^{13}C MAS spectra of the ^{13}CO -enriched black solid at 12 kHz spinning rate with a direct excitation method. Fitting of the peak at 94 ppm was necessary because overlapping of the Cp signal and the first order spinning sideband of the terminal CO signal occurred. The calculated ratio of bridging and terminal COs is 3:1.

7. Elemental Analysis and Electron Microprobe Analysis (EMPA)

Standard CHN elemental analysis (Elementar 4.1 vario EL 3) of the black solid gave reproducible contents of carbon, hydrogen and nitrogen with the following mean values (%): C 23.72, H 1.54, N 0.49. The low content of nitrogen can be traced back to residual amounts of the solvent MeCN as a batch of the black solid where we refrained from washing the raw product with MeCN did not contain any nitrogen impurities. However, as became clear from solid state NMR measurements, other impurities were present in this batch of the black solid. We were unable to remove the traces of MeCN by prolonged drying of the compound in vacuo. The content of ruthenium was determined photometrically (Perkin-Elmer Lambda 2) after pressure digestion with HNO₃ to be 42.26 %. ICP-OES measurements (Thermo Scientific IRIS Intrepid II) revealed a potassium content of 13.18 %.

Wavelength dispersive electron microprobe analysis (EMPA) was conducted using a JEOL JXA8900 RL instrument. The beam conditions were set to an accelerating voltage of 15 kV, a beam current of 15 nA, and a slightly defocussed beam of 5 μm diameter. The standards MgO (synthetic), sanidine (KAlSi₃O₈), wollastonite (CaSiO₃) and Ru metal were chosen to calibrate O, K, Si and Ru respectively. Matrix correction was performed using the $\Phi\rho z$ - method (CITZAF program) after Armstrong (1995).¹⁰

Quantification for Ru, K, O and Si at different positions of the sample revealed an average atomic ratio Ru:K:O of 4:3:8. The relatively low contents of Si can be attributed to impurities (e. g. silicon grease). Furthermore, the absolute contents of Ru (43.2 %) and K (13.0) largely confirm the values obtained before by other methods (see above). Details of the measurements can be found in Table S2. Recalculating the raw data using CITZAF and assuming that the unassigned content is carbon, leads to minor deviations represented as well in Table S2 ($\emptyset_{\text{C-calc}}$). Here, the 4:3 ratio of Ru:K is even more evident than without taking carbon into account. A direct determination of the carbon content was not possible due to the inadequate surface quality of the powdered sample which did not fulfill the requirements for a quantitative light element analysis. Taking together all experimentally determined values, 96.6 % of the elemental composition has been assigned.

Table S2: Details of EMPA measurements.

No.	mass percentage (wt%)					normalized atomic percentage (at%)					standard deviations (relative %) (1-sigma by counting statistics)			
	O	Si	Ru	K	total	O	Si	Ru	K	total	O	Si	Ru	K
1	11.8	0.6	44.0	14.1	70.5	47.4	1.4	28.0	23.2	100.0	1.41	2.23	0.67	0.62
2	12.0	0.8	43.9	12.8	69.5	48.6	1.9	28.2	21.3	100.0	1.40	1.81	0.67	0.65
3	12.6	0.4	45.6	13.2	71.9	49.6	1.0	28.3	21.2	100.0	1.36	2.87	0.66	0.64
4	11.7	0.5	44.4	14.2	70.8	47.3	1.0	28.3	23.4	100.0	1.42	2.70	0.66	0.62
5	13.1	0.8	43.1	12.7	69.7	51.3	1.8	26.6	20.3	100.0	1.32	1.79	0.68	0.65
6	14.8	0.5	43.6	12.4	71.3	54.7	1.1	25.5	18.8	100.0	1.23	2.45	0.67	0.66
7	18.0	1.3	40.6	12.7	72.5	59.3	2.4	21.2	17.1	100.0	1.07	1.38	0.70	0.65
8	14.6	0.7	41.8	13.0	70.1	54.1	1.5	24.6	19.8	100.0	1.23	1.99	0.69	0.64
9	13.2	0.5	43.1	12.9	69.7	51.5	1.2	26.7	20.6	100.0	1.31	2.39	0.68	0.65
10	17.4	0.9	41.6	12.6	72.4	58.7	1.7	22.3	17.4	100.0	1.09	1.74	0.69	0.65
11	14.7	0.6	43.9	12.2	71.4	54.4	1.3	25.8	18.6	100.0	1.22	2.21	0.67	0.66
\emptyset	14.0	0.7	43.2	13.0	70.9	52.4	1.5	26.0	20.2	100.0	1.28	2.14	0.68	0.64
$\emptyset_{\text{C-calc}}$	13.6	0.7	44.2	12.9	100.0	21.1	0.6	10.9	8.2	100.0	1.28	2.14	0.68	0.64

8. References

- (1) Fulmer, G. R.; Miller, A. J. M.; Sherden, N. H.; Gottlieb, H. E.; Nudelman, A.; Stoltz, B. M.; Bercaw, J. E.; Goldberg, K. I. *Organometallics* **2010**, *29*, 2176–2179.
- (2) Doherty, N. M.; Knox, S. A. R.; Morris, M. J. *Inorg. Syn.* **1990**, *28*, 189–191.
- (3) Darensbourg, D. J.; Gray, R. L.; Pala, M. *Organometallics* **1984**, *3*, 1928–1930.
- (4) G. M. Sheldrick, *Acta Cryst.* **2008**, *A64*, 112–122.
- (5) STOE & CIE GmbH, X-RED, Darmstadt (Germany), **2002**.
- (6) For IR spectra of HRp ($\tilde{\nu}(\text{CO}) = 2033\text{--}2022$ and $1973\text{--}1959\text{ cm}^{-1}$), see for example: (a) Davison, A.; McCleverty, J. A.; Wilkinson, G. *J. Chem. Soc.* **1963**, 1133–1138. (b) Estes, D. P.; Vannucci, A. K.; Hall, A. R.; Lichtenberger, D. L.; Norton, J. R. *Organometallics* **2011**, *30*, 3444–3447. (c) Humphries, A. P.; Knox, S. A. R. *J. Chem. Soc., Dalt. Trans.* **1975**, 1710–1714. (d) Bitterwolf, T. E.; Linehan, J. C.; Shade, J. E. *Organometallics* **2001**, *20*, 775–781.
- (7) Blackmore, T.; Cotton, J. D.; Bruce, M. I.; Stone, F. G. A. *J. Chem. Soc. A* **1968**, 2931–2936.
- (8) Krause, J. A.; Siriwardane, U.; Salupo, T. A.; Wermer, J. R.; Knoepfel, D. W.; Shore, S. G. *J. Organomet. Chem.* **1993**, *454*, 263–271.
- (9) Wojdyr, M. *J. Appl. Cryst.* **2010**, *43*, 1126–1128.
- (10) CITZAF: A package of correction programs for the quantitative electron microbeam X-ray analysis of thick polished materials, thin films, and particles. Armstrong, J. T. *Microbeam Anal.* **1995**, *4*, 177–200.